JOURNAL OF AGRICULTURAL AND FOOD CHEMISTRY

Determination and Applications of the Molar Absorptivity of Phenolic Adducts with Captopril and Mesna

F. García-Molina,[†] J. L. Muñoz-Muñoz,[†] M. García-Molina,[†] M. Molina-Alarcon,[‡] P. A. García-Ruíz,[§] J. Tudela,[†] and J. N. Rodríguez-López*,[†]

GENZ, Grupo de Investigación de Enzimología (http://www.um.es/genz), Departamento de Bioquímica y Biología Molecular-A, Facultad de Biología, Universidad de Murcia, A. Correos 4021, E-30080 Murcia, Spain, Departamento de Enfermería, Escuela Universitaria de Enfermería, Universidad de Castilla la Mancha, E-02071 Albacete, Spain, and QCBA, Grupo de Química de Carbohidratos y Biotecnología de Alimentos, Departamento de Química Orgánica, Facultad de Química, Universidad de Murcia, E-30100, Espinardo, Murcia, Spain

Captopril and mesna are molecules with a free thiol group, used as active ingredients due to their hypotensor and mucolytic properties, respectively. These compounds cross the hematoencephalic barrier and, due to the reactivity of their thiol group, can form adducts with the *o*-quinones formed during the oxidation of mono- and *o*-diphenols. Polyphenol oxidase from plants and fungi can be used as a tool for generating *o*-quinones in their action on *o*-diphenols and facilitate the formation of adducts in the presence of captopril or mesna. The spectrophotometric characterization of these adducts is useful from several points of view. Here, using the end-point method, which involves the exhaustion of oxygen in the medium, we determined the molar absorptivity of the adducts of different *o*-diphenols with captopril and mesna. Besides the analytical interest of this approach, we also use it to make a kinetic characterization of polyphenol oxidase as it acts on *o*-diphenolic substrates that produce unstable *o*-quinones.

KEYWORDS: polyphenol oxidase; captopril; mesna; thiol−diphenol adduct

INTRODUCTION

o-Diphenol oxidation by dissolved oxygen can be catalyzed enzymatically or nonenzymatically (autoxidation). The enzyme classically associated with *o*-diphenol oxidation is tyrosinase or polyphenol oxidase (PPO), an enzyme widely distributed across the phylogenetic scale. In humans, it is found in skin, eyes, and other locations, although there is controversy concerning whether or not it is found in brain (*1*−*3*).

All the *o*-quinones derived from the oxidation of monophenols and *o*-diphenols are unstable and susceptible to external nucleophilic additions, especially in the C5, C2, and C6 positions, where adducts are formed (*4*). The thiol groups of amino acids, such as cysteine and glutathione, are 3−4 orders of magnitude more reactive than amino nucleophilic groups (*5*). Indeed, the thiolate group is added to *o*-quinones even more rapidly than *o*-quinones are reduced by ascorbate (*5*). The addition of an external nucleophile transforms *o*-quinones to a substituted catechol (e.g., the addition of cysteine to the *o*-quinone of dopamine (DA) gives cysteinyldopamine (5-*S*-cysteinyl-DA) (*6*−*8*). Furthermore, thiols are time-dependent inhibitors of tyrosinase (*9*−*11*).

These reactions also have a possible physiopathological effect since some products derived from *o*-quinones, such as neuromelanins, have been identified in the nigrostriatal tissue, while thiol−catechol (adducts), among them 5-*S*-cysteinyl-DA and 5-*S*-cysteinyl-3,4-dihydroxyphenylacetic acid (5-*S*-cysteinyl-DOPAC)), have been found in human substantia nigra and striatum (*12, 13*). These adducts increase in concentration with age and in the face of degenerative lesions, among other causes (*12, 14*−*16*). The substantia nigra, particularly, undergoes oxidative change with age (*17*). The production of reactive oxygen species (ROS) can lead to secondary cytotoxicity through mitochondrial respiration or from alterations in the mitochondrial thiol pool. Both abnormalities have been recorded in Parkinsonian patients (*17*−*19*). Montine et al. (*20*) tested the toxicity of nine adducts on dopaminergic cells and found that only 5-*S*-cysteinil-DOPAC was neurotoxic.

However, Spencer et al. (*21*) described how the exposure of neurons to the 5-*S*-conjugates of DA, L-DOPA (3.4-dihydroxyphenylalanine), DOPAC, DHMA (dihydroxymandelic acid) (see

* Corresponding author. Fax: +34 968 364147. E-mail address: neptuno@um.es.
[†] Facultad de Biología, Universidad de Murcia.
[‡] Universidad de Castilla la Mancha.
[§] Facultad de Química, Universidad de Murcia.

10.1021/jf803447g CCC: $40.75
Published on Web 01/26/2009

Scheme 1. Chemical Structure of the Thiols Used in This Study

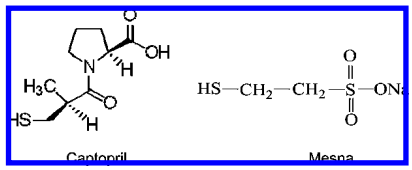

Material and Methods), produced neuronal damage, increased the oxidation of DNA, and stimulated caspase-3 activity in cells, the adduct being capable of entering the cell and stimulating the action of caspases (*21*). Subsequently, the existence of tyrosinase in the brain and the level of cell death was demonstrated (*22*). Because both captopril and mesna (sodium-2-mercaptoethanesulfonate, **Scheme 1**) cross the hematoencephalic barrier (*23*−*25*), the *in vivo* formation of adducts is probably possible in the same way as they are formed *in vitro*.

In contrast, a multiple function for angiotensin II has recently been demonstrated in brain (*26*), including regulation of DA release from the striatum nucleus. Active angiotensin is an NADPH-dependent oxidase, which acts as a source of superoxide anion. Inhibitors of angiotensin conversion show antioxidant properties in several tissues. The above authors carried out an assay with a widely validated model of Parkinson's disease, which consisted of intraventricular injection of 6-hydroxydopamine to generate oxidative stress in the dopaminergic system. The rats receiving captopril showed less neuronal death than controls. Captopril also reduced all the indices of oxidative stress (lipid peroxidation, etc.) (*27*).

Knowledge of the molar absorptivities of thiol−diphenol adduct may be of interest for quantifying these compounds in biological samples (*28*−*31*). In order to calculate the molar absorptivities of the thiol−diphenol adduct, we have developed a method based on the stoichiometric depletion of oxygen in the oxidation of *o*-diphenol by mushroom PPO and the capacity the thiol group to trap the *o*-quinones generated (*32*). In this paper, we apply the method to determine the molar absorptivities of thiol−diphenol adducts of the thiol drugs captopril and mesna with *o*-quinones from several *o*-diphenols and catecholamines.

Mesna (**Scheme 1**) is a thiol drug that acts as a mucolytic and can also be used to eliminate contrast in bronchographs. Mesna functions as a regional detoxifying agent of urotoxic ifosfamide metabolites such as acrolein, 4-hydroxy-ifosfamide, and chloroacetaldehyde (*33*). The resulting free thiol group of mesna can combine directly with the double bond of acrolein or with other toxic oxazaphosphorine metabolites in the bladder to form stable and nontoxic compounds (*34*).

Captopril (**Scheme 1**) has an antihypertensive effect. It is effective alone or in combination with other antihypertensive agents, especially thiazide diuretics, when the overall effect is practically additive. Captopril can also be used to treat cardiac insufficiency.

The objective of the present work was to characterize the molar absorptivities of the adducts of mesna and captopril with the *o*-quinones of *o*-diphenols or with metabolites (neurotransmitters) such as dopamine, adrenaline, or noradrenaline (NA) or drugs such as L-DOPA (antiparkinsonian) and α-methyl-DOPA (antihypertensive).

The calculation of the molar absorptivity of the adducts can be of use for the quantitative determination of the adducts as well for determining the enzymatic activity when PPO acts on *o*-diphenols that originate very unstable *o*-quinones, although, in this last case, it must be demonstrated that the initial velocity measurements (when $t \rightarrow 0$) are not affected by the presence of the thiol.

Table 1. Molar Absorptivities of *o*-Diphenols and Thiol−Diphenol Adducts at $\lambda = 300$ nm

	ε_{300} (M^{-1} cm^{-1})		
o-diphenol	captopril−diphenol adduct	mesna−diphenol adduct	*o*-diphenol
Cat	1835	1613	20
DOPAC	1926	2230	40
DHPPA	1995	1278	50
DHMA	2031	1586	7
dopamine	2795	1831	66
adrenaline	2447	1465	95
epinine	2645	1952	100
4MeCat	1382	4147	50
L-αMeDOPA	3227	1468	60
L-DOPA	3120	1340	58
L-DOPAMeE	1695	1550	110
L-IsoProt	2303	1663	150
NA	2360	1324	81
TBC	2442	2341	32

Scheme 2

$$2D + O_2 \xrightarrow{PPO} 2Q + 2H_2O$$

MATERIALS AND METHODS

Reagents. Mushroom PPO (5350 units/mg) was purchased from Sigma and was purified as described by Rodríguez-Lopez et al. (*35*). Protein concentrations were determined by Bradford's method using bovine serum albumin as a standard (*36*). Catechol (Cat) and noradrenaline (NA) were purchased from Fluka (Spain), while mesna (2-mercaptoethanesulfonic acid), captopril, (*N*-[(*S*)-3-mercapto-2-methylpropionyl]-L-proline), 4-methylcatechol (4-MeCat), 3,4-dihydroxymandelic acid (DHMA), 3,4-dihydroxyphenylpropionic acid (DHPPA), 3,4-dihydroxyphenylacetic acid (DOPAC), L-DOPA, L-α-methylDOPA (L-α-MeDOPA), epinine, L-DOPA methyl ester (L-DOPAMeE), L-isoprotenerol (L-IsoProt), adrenaline (A), and dopamine (DA) were purchased from Sigma (St. Louis, MO). 4-*tert*-Butylcatechol (TBC) was purchased from Across Organics (Belgium). Stock solutions of phenolic substrates were prepared in 0.15 mM phosphoric acid in order to prevent autoxidation. Milli-Q system (Millipore Corp.) ultrapure water was used throughout this research.

Spectrophotometric Assays. In the assays of PPO with *o*-diphenolic substrates in the presence of thiols, the formation of thiol−diphenol adducts was followed at 300 nm. (see **Table 1**). Assays were carried out on a Perkin-Elmer Lambda-35 spectrophotometer interfaced to a PC-compatible computer running Perkin-Elmer UV-Winlab software. The standard assay contained *o*-diphenol (2 mM) and thiol (2 mM) in 30 mM phosphate buffer, pH 7.0, through which nitrogen gas was bubbled prior to use. The reaction was started by injection of enzyme (50−100 nM per sample) containing a known concentration of oxygen (10−110 μM). The cuvette was then rapidly closed with a Teflon stopper. The spectrophotometric signal was determined by recording the increase in absorbance, which values are included in the following equation:

$$A_\lambda = 2[\varepsilon_\lambda^{\text{adduct}} - \varepsilon_\lambda^{o\text{-diphenol}}][O_2]_0 + \varepsilon_\lambda^{o\text{-diphenol}}[D]_0 + A_\lambda^{\text{PPO}} \quad (1)$$

where A_λ is the absorbance obtained experimentally, $[D]_0$ is the initial concentration of *o*-diphenol, and $[O_2]_0$ is the initial concentration of oxygen used in each experiment, as determined by the above-described method (*37*). Knowing the molar absorptivities of the *o*-diphenol at this wavelength, one can obtain the molar absorptivities of the adduct from the slope of the eq 1. To measure the enzymatic activity, the slope of eq 1 can be used and the initial velocity can be calculated (μmol/min or IU).

Oximetric Assays. The O_2 concentration was determined by using a Clark electrode with a Hansatech Oxygraph (Kings Lynn, UK), interfaced to a PC-compatible computer running Quiceltron software. The equipment was calibrated using the tyrosinase/4-*tert*-butylcatechol method (*37*).

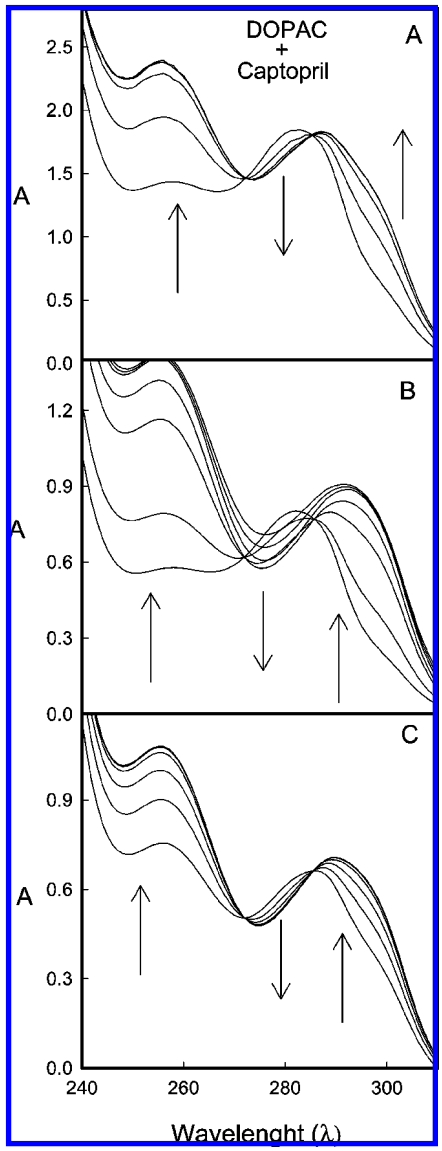

Figure 1. (**A**) Spectra obtained during the oxidation of DOPAC by mushroom PPO in the presence of captopril. The reaction mixture contained $[DOPAC]_0 = 0.7$ mM, $[O_2]_0 = 0.26$ mM, $[captopril]_0 = 1$ mM, and $[E]_0 = 75.9$ nM in 30 mM sodium phosphate buffer, pH 7.0, at 25 °C. The difference in time between each spectrum was 20 s. (**B**) *o*-Diphenol depletion. The assay conditions were $[DOPAC]_0 = 0.3$ mM, $[O_2]_0 = 0.26$ mM, $[PPO]_0 = 75.9$ nM, $[captopril]_0 = 1$ mM in 30 mM sodium phosphate buffer, pH 7.0, at 25 °C. The difference between the first four spectra was 15 s and that between the last three 40 min. (**C**) Oxygen depletion. The assay conditions were $[DOPAC]_0 = 0.3$ mM, $[O_2]_0 = 0.125$ mM, $[PPO]_0 = 83.5$ nM in the presence of $[captopril]_0 = 1$ mM in 30 mM sodium phosphate buffer, pH 7.0, at 25 °C. The difference between the first six spectra was 50 s, while the last spectrum was obtained after 1 h.

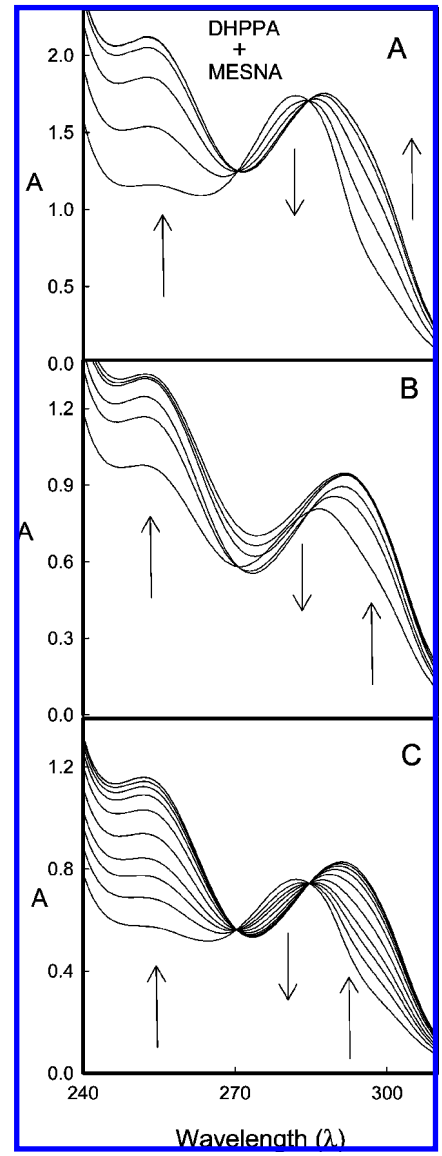

Figure 2. (**A**) Spectra obtained during the oxidation of DHPPA by mushroom PPO in the presence of mesna. The reaction mixture contained $[DHPPA]_0 = 0.7$ mM, $[O_2]_0 = 0.26$ mM, $[mesna]_0 = 1$ mM, and $[E]_0 = 20$ nM. The assay conditions were 30 mM sodium phosphate buffer, pH 7.0, at 25 °C. The difference in time between successive spectra was 20 s. (**B**) *o*-Diphenol depletion. The reaction mixture contained $[DHPPA]_0 = 0.3$ mM, $[O]_2 = 0.26$ mM, $[PPO]_0 = 58.2$ nM, and $[mesna]_0 = 1$ mM. The assay conditions were 30 mM sodium phosphate buffer, pH 7.0, at 25 °C. The difference in time between successive spectra was 30 s for the first three, 30 min between the third and fourth, and 15 min between the last three. (**C**) Oxygen depletion. The reaction mixture contained $[DHPPA]_0 = 0.3$ mM, $[O]_2 = 0.13$ mM, $[PPO]_0 = 17$ nM, and $[mesna]_0 = 1$ mM. The assay conditions were 30 mM sodium phosphate buffer, pH 7.0, at 25 °C. The difference between successive spectra was 25 s for the first six and 50 s between the following four. The last spectrum was obtained after 1 h.

^{13}C NMR Assays. ^{13}C NMR spectra of thiols were obtained at pH 7.0 on a Varian Unity spectrophotometer (300 MHz) using deuterated water as solvent. Chemical-shift values (δ) were measured relative to those for tetramethylsilane ($\delta = 0$). The maximum accepted error for each peak was ± 0.03 ppm.

HPLC Assays. Adduct was formed between mesna and *o*-dopaquinone by the reaction with 2 mM L-DOPA, 2 mM mesna, and 100 nM PPO in 30 mM sodium phosphate buffer, pH 7.0, at 25 °C, in an oxygen concentration of 0.13 mM. After 30 s, when the reaction had subsided,10 M HCl was added to reach a pH of 1.5 and 40 μL of the mixture was injected in a VWR Hitachi Elite Lachrom chromatograph equipped with an L-2130 pump and L-2455 diode array detector. The column used was a Teknokroma Mediterranea Sea C-18 measuring 25 cm $\times$ 0.40 cm and 5 μm particle size. The mobile phase was composed of (A) 2.9 g/L phosphoric acid and 6.0 g/L metasulfonic acid in water and (B) 100% acetonitrile. The analysis were made with the following gradient: 100% A (0 min), 30% B (15−25 min), and 100% A (30 min). This phase was pumped through the system at a flow rate of 1.0 mL/min.

MS experiments were performed using a Agilent VL mass spectrometer. Ionization was achieved using standard electrospray (ESI)

Scheme 3. Enzymatic and Nonenzymatic Reactions Related to the Oxidation by O_2 of *o*-Diphenols Catalyzed by PPO in the Presence of Thiol Compounds

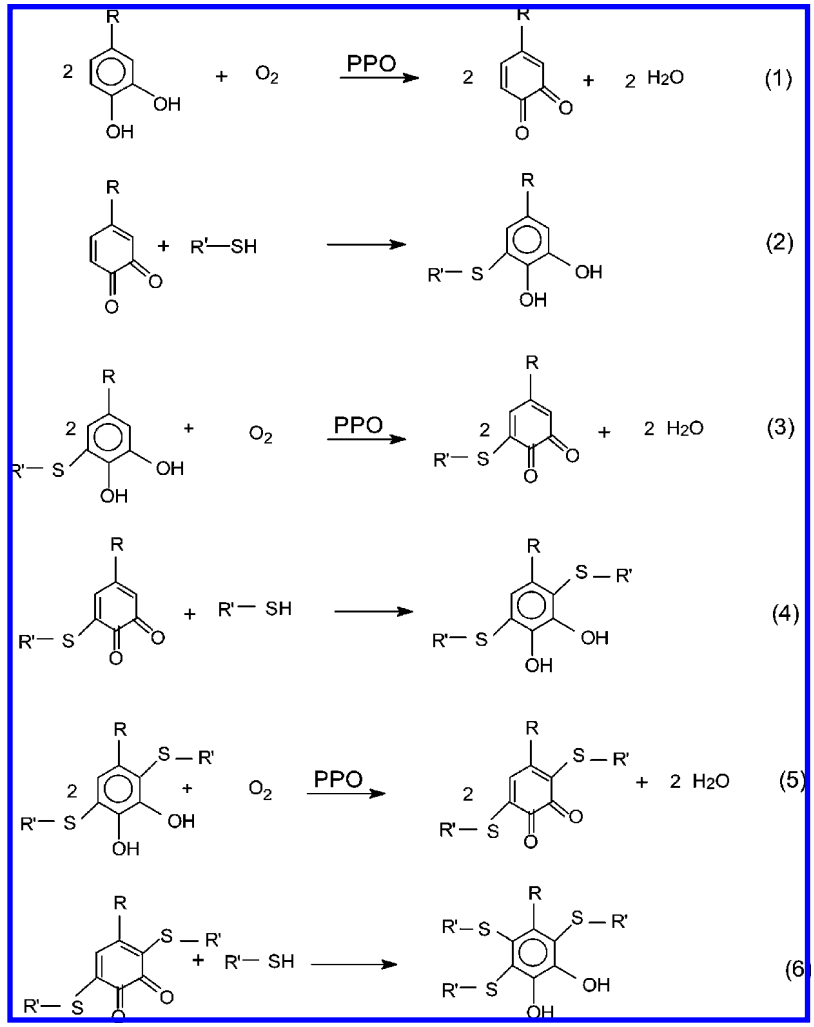

conditions and data were adquired in both positive and negative ion modes. Source temperature was 350 °C and capillary voltage was set at ±105 V. Mass spectra were recorded from 100 to 500 amu. The sample was diluted approximately 10-fold in methanol containing 0.1% formic acid and infused into the mass spectrometer using a 100 μL Hamilton syringe.

RESULTS AND DISCUSSION

Stoichiometric Considerations. The reaction of PPO with *o*-diphenols can be represented as depicted in **Scheme 2** (*35*). The mechanism shown in **Scheme 2** indicates that the rate of *o*-quinone formation (V_{ss}^{Q}) is double the rate of oxygen consumption ($V_{ss}^{O_2}$) and so the stoichiometry of the reaction is $1O_2$/2Q, as demonstrated previously (*35*).

When *o*-diphenols are oxidized in the presence of compounds containing a thiol group, the deprotonated thiol group ($R-S^-$) attacks the *o*-quinone generated by the enzyme in a powerful nucleophilic attack that prevents the accumulation of *o*-quinone in the reaction medium, as demonstrated by the isosbestic points generated during the oxidation of NA in the presence of captopril or mesna (**Figures 1A** and **2A**, respectively). Therefore, there is a specific stoichiometry for the transformation of a diphenol to adduct (thiol−diphenol). According to **Scheme 2**, this stoichiometry is one O_2 oxidizing two *o*-diphenols, producing two *o*-quinones and so two adducts (thiol−diphenol).

The adducts (thiol−diphenol) are not sold, so their spectral characteristics are not available for their characterization in biological samples where it would be of interest to detect their presence. An important physical−chemical property of the adduct is the molar absorptivity in the zone of the spectrum where it most differs from the *o*-diphenol that produces it. The adduct can be determined from the activity of PPO on different *o*-diphenols in the presence of the thiol compound. There are two experimental strategies possible since this enzyme is bisubstrate: exhaustion of the concentration of *o*-diphenol or exhaustion of the concentration of oxygen.

Below we describe these approaches kinetically.

Diphenol Exhaustion. If $[O_2]_0 \gg [D]_0$ and saturating, the rate of *o*-quinone formation of PPO acting on D (**Scheme 2**) is

$$V_{ss}^{Q} = \frac{V_{max}^{Q}[D]_0}{K_m^D + [D]_0} \quad (2)$$

If $[D]_0 \ll K_m^D$, eq 2 is transformed into

$$V_{ss}^{Q} = \frac{V_{max}^{Q}}{K_m^D}[D]_0 \quad (3)$$

The apparent first-order constant (k_{app}) of this transformation is

$$k_{app} = \frac{V_{max}^{Q}}{K_m^D} = \frac{2k_{cat}^D[E]_0}{K_m^D} \quad (4)$$

so that, in accordance with eq 4, the rate of the process depends on the concentration of enzyme. However, this *o*-diphenol

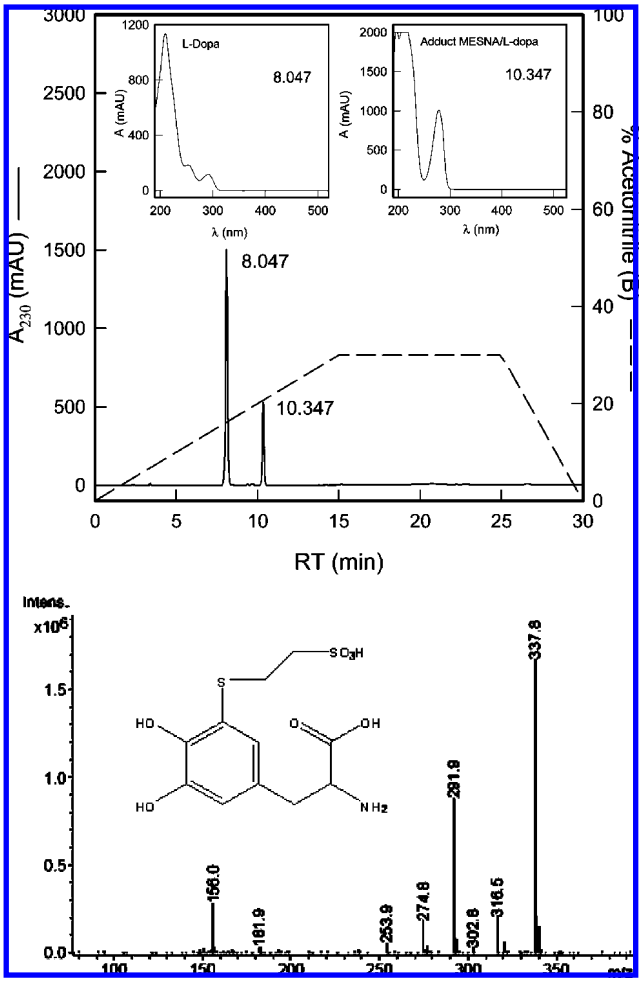

Figure 3. (**A**) Chromatograms of a reaction between L-DOPA and PPO in the presence of mesna. The experimental conditions were 30 mM phosphate buffer, pH 7.0, at 25 °C, $[\text{L-DOPA}]_0 = 2$ mM, $[\text{mesna}]_0 = 2$ mM, $[\text{PPO}]_0 = 100$ nM, and $[O_2] = 0.13$ mM. The reaction was carried out as described in Materials and Methods: L-DOPA ($t_R = 8.047$), adduct 5-*S*-mercaptoethanesulfonil-DOPA ($t_R = 10.347$). Inset of $t_R = 8.047$ shows the UV−visible spectrum of L-DOPA and that of $t_R = 10.347$ shows UV−visible spectrum of the adduct. (**B**) MS experiment on 5-*S*-mercaptoethanesulfonil−DOPA. Mass spectra were recorded in positive ion mode and showed the 5-*S*-mercaptoethanesulfonil−DOPA and its major fragments.

exhaustion method has the disadvantage that the enzyme attacks the monoadducts again, giving rise to di- and triadducts, as shown in **Scheme 3**. This is seen from the fact that the isosbestic points are broken during the enzymatic oxidation (**Figures 1B** and **2B** for captopril and mesna, respectively). For this reason, in this study, we propose using PPO in limiting oxygen conditions until all the oxygen is used up (see below).

Oxygen Exhaustion. The action of PPO (**Scheme 2**), if the concentration of oxygen is $[O_2]_0 \ll [D]_0$ and *o*-diphenol is saturating, is as follows:

$$V_{ss}^{Q} = \frac{V_{max}^{Q}[O_2]_0}{K_m^{O_2} + [O_2]_0} \tag{5}$$

When the concentration of oxygen is low so that $[O_2]_0 \ll K_m^{O_2}$, eq 5 can be simplified to

$$V_{ss}^{Q} = \frac{V_{max}^{Q}}{K_m^{O_2}}[O_2]_0 = \frac{2k_{cat}^{D}[E_0]}{K_m^{O_2}}[O_2]_0 \tag{6}$$

In this case, the apparent first-order constant, k_{app}', is

$$k'_{app} = \frac{2k_{cat}^{D}[E]_0}{K_m^{O_2}} \tag{7}$$

Since $K_m^{O_2}$ (μM) $\ll K_m^{D}$ (mM), from eq 4 and eq 7, it results that

$$k'_{app} \gg k_{app} \tag{8}$$

That is, this approach leads to a much more rapid exhaustion of the reaction since the oxygen is used up during the formation of the monoadducts, so reactions 3−6 of **Scheme 3** do not take place.

The experimental approach involving the exhaustion of *o*-diphenol leads to both isosbestic points being broken, as is evident from **Figures 1B** and **2B**, while exhaustion of the oxygen means that the isosbestic points are maintained (**Figures 1C** and **2C**). This means that while di- and triadducts are formed in the first place, almost only one species exists in the second,

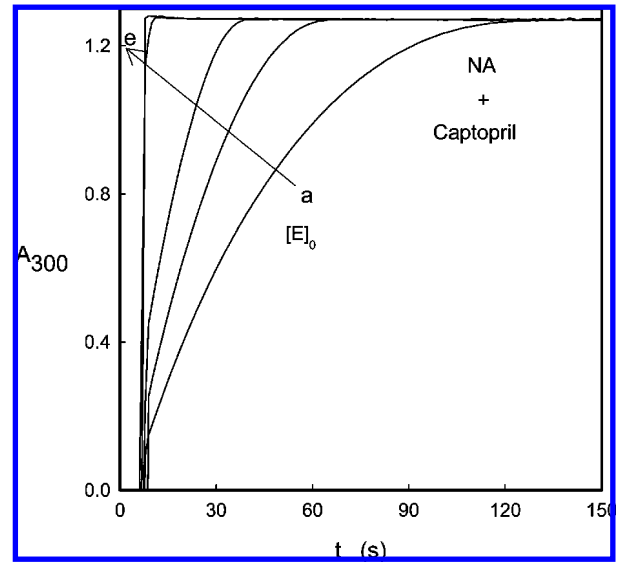

Figure 4. Progress curves at 300 nm of the formation of the NA−captopril adduct. Assay conditions were $[\text{NA}]_0 = 1.2$ mM, $[O_2]_0 = 0.26$ mM, and $[\text{captopril}]_0 = 2$ mM in 30 mM sodium phosphate buffer, pH 7.0, at 25 °C and $[E]_0 = 24$ (a), 36 (b), 48 (c), 60 (d), and 72 nM (e), respectively.

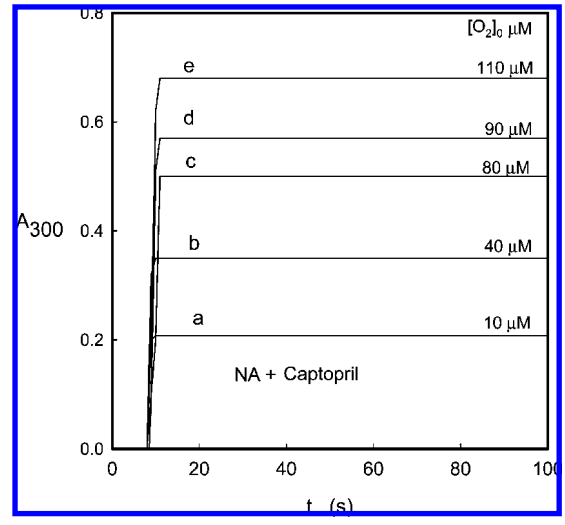

Figure 5. Progress curves at 300 nm used to calculate the molar absorptivities of adducts considering that 1 $O_2 = 2$ adducts: $[\text{captopril}]_0 = 2$ mM, $[E]_0 = 60$ nM, and $[\text{NA}]_0 = 2$ mM in 30 mM sodium phosphate buffer, pH 7.0, at 25 °C. $[O_2]_0 = 10$ (a), 40 (b), 80 (c), 90 (d), and 110 μM (e), respectively.

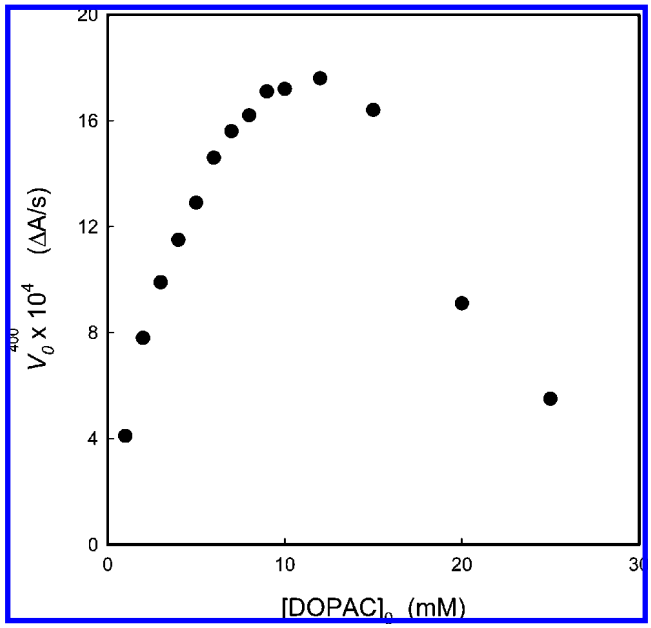

Figure 6. Representation of the initial rate (V_0) of *o*-quinone formation ($\lambda = 400$ nm) during the oxidation of DOPAC by PPO. Assay conditions were $[E]_0 = 2$ nM, $[O_2] = 0.26$ mM in 30 mM sodium phosphate buffer, pH 7.0, at 25 °C.

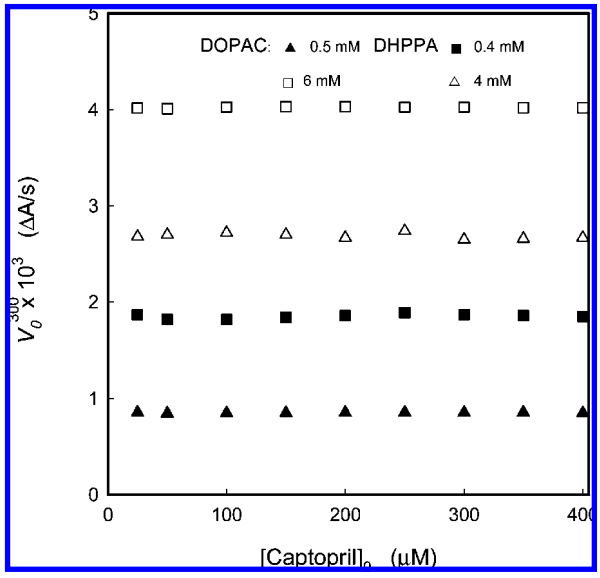

Figure 7. Representation of the initial rates of captopril adduct formation ($\lambda = 300$ nm) during the oxidation of DOPAC and DHPPA by PPO at different thiol concentrations. Assay conditions were 30 mM sodium phosphate buffer, pH 7.0, at 25 °C, $[E]_0 = 2$ nM; $[DOPAC]_0$ were (▲) 0.5 mM and (□) 6 mM; $[DHPPA]_0$ were (■) 0.4 mM and (△) 4.0 mM.

the monoadduct (**Scheme 3**). Furthermore, this result can be confirmed by HPLC experiments (**Figure 3**). When working in these conditions (limiting oxygen), injection of a reaction sample into the chromatograph gives two peaks corresponding to *o*-difenol in excess and the adduct formed (**Figure 3**).

Measurement Wavelength. To calculate the molar absorptivity of the adduct formed in the zone where it most differs from the corresponding *o*-diphenol, 300 nm was chosen.

Effect of enzyme concentration. With a saturating concentration of *o*-diphenol, the quantity of enzyme was varied. As **Figure 4** shows, the recorded rate increased with increasing concentrations of enzyme, which agrees with eq 6.

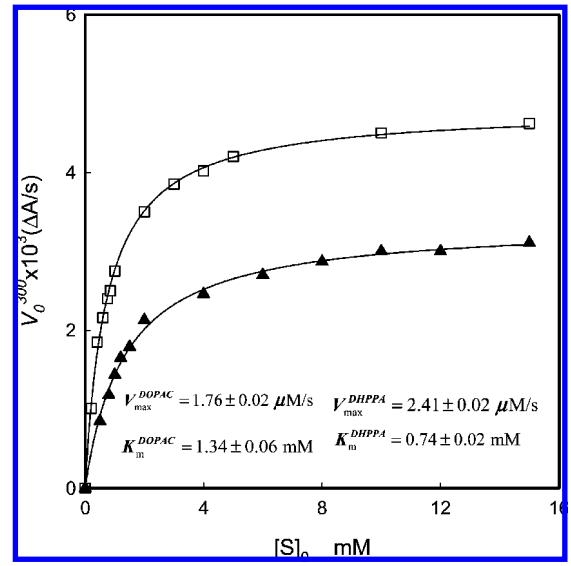

Figure 8. Representation of the initial rates of captopril adduct formation ($\lambda = 300$ nm) during the oxidation of DOPAC and DHPPA by PPO, obtaining V_{max} and K_m. The experimental conditions were 30 mM pH 7.0 phosphate buffer at 25 °C, $[E]_0 = 2$ nM, and $[captopril]_0 = 0.3$ mM: (▲) [DOPAC]; (□) [DHPPA]. The values of V_{max} and K_m are shown for each substrate.

Nucleophilic Characteristics of the Thiols Used. From the ^{13}C NMR spectra, the δ values of the carbon that supports the thiol group were obtained (captopril $\delta = 41.80$ and mesna $\delta = 17.96$), the lower δ value of the mesna reflecting its stronger nucleophilic nature. These observations agree with the pK_a of the thiol groups, 9.8 for captopril and 9.06 for mesna. Since an end point method is being used, the possible inhibition of PPO by the thiol would not affect the method.

Effect of Oxygen Concentration and Calculation of the Molar Absorptivity Coefficient. In conditions of limiting oxygen and maintainance of a fixed substrate and enzyme concentration, the oxygen concentration was varied. The corresponding recordings are shown in **Figure 5**. The absorbancies obtained with the oxygen concentrations assayed fit to eq 1. In the experimental conditions of 30 mM sodium phosphate buffer, pH 7.0, at 25 °C, $[E]_0 = 60$ nM, $[NA]_0 = 2$ mM, and $[captopril]_0 = 2$ mM, the following equation was obtained:

$$A_{300} = \{(4.56 \pm 0.22) \times 10^{-3}\}[O_2]_0 + (0.17 \pm 0.01) \quad (9)$$

Table 1 shows the molar absorptivity values (ε_{300}) obtained for the adducts of different *o*-diphenols with captopril and mesna using the same methodology. In general, the values of ε_{300} obtained for the former are higher due to the presence of an imidazole ring in captopril, which is of interest when determining these adducts.

Application to the Measurement of PPO Activity. Measuring adduct formation can be useful for the kinetic characterization of substrates (*o*-diphenols) of the enzyme, as shown by the following experiments. **Figure 6** shows how measuring *o*-quinone formation from the oxidation of DHPPA points to the apparent inhibition by excess of substrate due to the reaction between *o*-quinone and *o*-diphenol or *o*-quinone and *o*-quinone although this can be prevented by adding a thiol (captopril or mesna) to the medium, generating the corresponding adducts. As indicated above, thiols are time-dependent inhibitors of PPO, but at low concentrations and measuring initial rates (when $t \rightarrow 0$), the inhibition does not occur in the case of DOPAC

and DHPPA (**Figure 7**). This means that in such conditions it is possible to measure V_0, and by analyzing the results depicted in **Figure 8**, it is possible to obtain V_{max} and K_m for these substrates (see **Figure 8**). These values agree with those previously obtained by other methods used to measure the enzymatic activity of PPO for these *o*-diphenols (*38*, *39*).

In conclusion, the end point method here described uses mushroom PPO, although PPO from any vegetal source can be used, in the enzymatic reaction that generates *o*-quinones. The method is useful for spectrophotometrically characterizing the adducts of the *o*-quinones of different *o*-diphenols with the thiols captopril and mesna. The method is based on the exhaustion of oxygen in the medium by means of the reaction of PPO. The usefulness of the molar absorptivity coefficient in analytic and kinetic assays is revealed by applying it to kinetically characterizing substrates of PPO, after checking in this case that the concentrations of thiol used do not inhibit the enzyme during initial velocity measurements ($t \rightarrow 0$).

ACKNOWLEDGMENT

The authors thank Dr. Francisco García Cánovas for checking the manuscript.

LITERATURE CITED

(1) Ikemoto, K.; Nagatsu, I.; Ito, S.; King, R. A.; Nishimura, A.; Nagatsu, T. Does tyrosinase exist in neuromelanin-pigmented neurons in the human substantia nigra. *Neurosci. Lett*. **1998**, *253*, 198–200.

(2) Xu, Y.; Stokes, A. H.; Freeman, W. M.; Kumer, S. C.; Vogt, B. A.; Vrana, K. E. Tyrosinase mRNA is expressed in human substantia nigra. *Brain Res. Mol. Brain Res*. **1997**, *45*, 159–162.

(3) Tief, K.; Schmidt, A.; Beermann, F. New evidence for presence of tyrosinase in substantia nigra, forebrain and midbrain. *Brain Res. Mol. Brain Res*. **1998**, *53*, 307–310.

(4) Ito, S.; Kato, T.; Fujita, K. Covalent binding of catechols to proteins through the sulphydryl group. *Biochem. Pharmacol*. **1988**, *37*, 1707–1710.

(5) Tse, D. C.; McCreery, R. L.; Adams, R. N. Potential oxidative pathways of brain catecholamines. *J. Med. Chem*. **1976**, *19*, 37–40.

(6) Shen, X. M.; Dryhurst, G. Further insights into the influence of L-cysteine on the oxidation chemistry of dopamine: Reaction pathways of potential relevance to Parkinson's disease. *Chem. Res. Toxicol*. **1996**, *9*, 751–763.

(7) Shen, X. M.; Zhang, F.; Dryhurst, G. Oxidation of dopamine in the presence of cysteine: Characterization of new toxic products. *Chem. Res. Toxicol*. **1997**, *10*, 147–155.

(8) Zhang, F.; Dryhurst, G. Effects of L-cysteine on the oxidation chemistry of dopamine: New reaction pathways of potential relevance to idiopathic Parkinson's disease. *J. Med. Chem*. **1994**, *37*, 1084–1098.

(9) Lerch, K.; Mims, W. B.; Peisach, J. Pulsed EPR studies of peroxide-activated cytochrome C peroxidase and of the mercaptoethanol derivative of *Neurospora* tyrosinase. *J. Biol. Chem*. **1981**, *256*, 10088–10091.

(10) Aasa, R.; Deinum, J.; Lerch, K.; Reinhammar, B. The reaction of mercaptans with tyrosinase and hemocyanins. *Biochim. Biophys. Acta* **1978**, *535*, 287–298.

(11) Valero, E.; Varón, R.; García-Carmona, F. A kinetic study of irreversible enzyme inhibition by an inhibitor that is rendered unstable by enzymic catalysis. The inhibition of polyphenol oxidase by L-cysteine. *Biochem. J*. **1991**, *277*, 869–874.

(12) Fornstedt, B.; Brun, A.; Rosengren, E.; Carlsson, A. The apparent autooxidaton rate of catechols in dopamine-rich regions of human brains increases with the degree of depigmentation of substantia nigra. *J. Neural Transm. Parkinson's Dis. Dementia Sect*. **1989**, *1*, 279–295.

(13) Fornstedt, B.; Rosengren, E.; Carlsson, A. Occurrence and distribution of 5-S-cysteinyl derivatives of dopamine, dopa and dopac in the brains of eight mammalian species. *Neuropharmacology*. **1986**, *25*, 451–454.

(14) Fornstedt, B.; Carlsson, A. Effects of inhibition of monoamine oxidase on the levels of 5-S-cysteinyl adducts of catechols in dopaminergic regions of the brains of the guinea pig. *Neuropharmacology*. **1991**, *30*, 463–468.

(15) Fornstedt, B.; Carlsson, A. Vitamin C deficiency facilitates 5-S-Cysteinyldopamine formation in guinea pig striatum. *J. Neurochem*. **1991**, *56*, 407–414.

(16) Fornstedt, B.; Pileblad, E.; Carlsson, A. In vivo autooxidation of dopamine in guinea pig striatum increases with age. *J. Neurochem*. **1990**, *55*, 655–659.

(17) Perry, T. L.; Godin, D. V.; Hansen, S. Parkinson's disease: A disorder due to nigral glutathione deficiency. *Neurosci. Lett*. **1982**, *33*, 305–310.

(18) Jenner, P. Oxidative stress in Parkinson's disease. *Ann. Neurol*. **2003**, *53* (Suppl 3), S26–38, Review.

(19) Schapira, A. H.; Hartley, A.; Cleeter, M. W.; Cooper, J. M. Free radicals and mitochondria dysfunction in Parkinson's disease. *Biochem. Soc. Trans*. **1993**, *21*, 367–370.

(20) Montine, T. J.; Picklo, M. J.; Amarnath, V., Jr.; Graham, D. G. Neurotoxicity of endogenous cysteinylcatechols. *Exp. Neurol*. **1997**, *148*, 26–33.

(21) Spencer, J. P.; Whiteman, M.; Jenner, P.; Halliwell, B. 5-S-Cysteinyl- conjugates of catecholamines induce cell damage extensive DNA base modification and increases in caspase-3 activity in neurons. *J. Neurochem*. **2002**, *81*, 122–129.

(22) Greggio, E.; Bergantino, E.; Carter, D.; Ahmad, R.; Costin, G. E.; Hearing, V. J.; Clarimon, J.; Singleton, A.; Eerola, J.; Hellström, O.; Tienari, P. J.; Miller, D. W.; Beilina, A.; Bubacco, L.; Cookson, M. R. Tyrosinase exacerbates dopamine toxicity but is not genetically associated with Parkinson's disease. *J. Neurochem*. **2005**, *93*, 246–256.

(23) Knopman, D. S. October 12 highlights and commentary. *Neurology* **2007**, *63*, 1145–1146.

(24) Ohrui, T.; Tomita, N.; Sato-Nakagawa, T.; Matsui, T.; Maruyama, M.; Niwa, K.; Arai, H.; Sasaki, H. Effects of brain-penetrating ACE inhibitors on Alzheimer disease progression. *Neurology* **2004**, *63*, 1324–1325.

(25) Mare, S.; Penugonda, S.; Ercal, N. High performance liquid chomatography analysis of MESNA (2-mercaptoethane sulfonate) in biological samples using fluorescence detection. *Biomed. Chromatogr*. **2005**, *19*, 80–86.

(26) Lopez-Real, A.; Rey, P.; Soto-Otero, R.; Mendez-Alvarez, E.; Labandeira-García, J. L. Angiotensin-converting enzyme inhibition reduces oxidative stress and protects dopaminergic neurons in a 6-hydroxydopamine rat model of Parkinsonism. *J. Neurosci. Res*. **2005**, *81*, 865–873.

(27) Muñoz, A.; Rey, P.; Guerra, M. J.; Mendez-Alvarez, E.; Soto-Otero, R.; Labandeira-García, J. L. Reduction of dopaminergic degeneration and oxidative stress by inhibition of angiotensin converting enzyme in a MPTP model of parkinsonism. *Neuropharmacology* **2006**, *51*, 112–120.

(28) Prota, G.; d'Ischia, M.; Napolitano, A. The Chemistry of Melanins and Related Metabolites. In *The Pigmentary System*; Nordlund, J. J., Boissy, R., Hearing, V., King, R., Ortonne, J. P., Eds.; University Press: Oxford, U.K., 1998; pp 307−332.

(29) Zawistowski, J.; Biliaderis, C. G.; Michael Eskin, N. A. Polyphenol Oxidase. In *Oxidative Enzymes in Foods*; Robinson D. S., Eskin N. A. M., Eds.; Elsevier Science: London, 1991, pp 217−273.

(30) Nicolas, J. J.; Richard-Forget, F.; Goupy, P. M.; Amiot, M. J.; Aubert, S. Y. Enzymatic browning reactions in apple and apple products. *CRC Crit. Rev. Food Sci*. **1994**, *34*, 109–157.

(31) Whitaker, J. R.; Lee, C. Y. Recent advances in chemistry of enzymatic browning: An overview. In *Enzymatic Browning and its Prevention*; Lee, C. Y., Whitaker, J. R., Eds.: American Chemical Society: Washington, DC, 1995.

(32) Peñalver, M. J.; Rodríguez-Lopez, J. N.; García Molina, F.; García Cánovas, F.; Tudela, J. Method for the determination of molar absorptivities of thiol adducts formed from diphenolic substrates of polyphenol oxidase. *Anal. Biochem.* **2002**, *309*, 180–185.

(33) Goren, M. P. Oral mesna: A review. *Semin. Oncol.* **1992**, *6* (Suppl 12), 65–67.

(34) Stofer-Vogel, B.; Cerny, T; Borner, M.; Lauterburg, B. H. Oral bioavailability of mesna tablets. *Cancer Chemother. Pharmacol.* **1993**, *32*, 78–81.

(35) Rodríguez-López, J. N.; Fenoll, L. G.; García-Ruíz, P. A.; Varón, R.; Tudela, J.; Thorneley, R. N.; García-Cánovas, F. Stopped-flow and steady-state study of the diphenolase activity of mushroom tyrosinase. *Biochemistry.* **2000**, *39*, 10497–10506.

(36) Bradford, M. M. A rapid and sensitive method for the quantification of microgram quantities of protein utilizing the principle of protein-dye binding. *Anal. Biochem.* **1976**, *72*, 248–254.

(37) Rodríguez-López, J. N.; Ros-Martínez, J. R.; Varón, R.; García-Cánovas, F. Calibration of a Clark-type oxygen electrode by tyrosinase-catalyzed oxidation of 4-*tert*-butylcatechol. *Anal. Biochem.* **1992**, *202*, 356–360.

(38) Muñoz, J. L.; García-Molina, F.; Varón, R.; Rodríguez-Lopez, J. N.; García-Cánovas, F.; Tudela, J. Calculating molar absorptivities for *o*-quinonas: application to the measurement of tyrosinase activity. *Anal. Biochem.* **2006**, *351*, 128–138.

(39) García-Molina, F.; Muñoz, J. L.; Varón, R.; Rodríguez-Lopez, J. N.; García-Cánovas, F.; Tudela, J. A review on spectrophotometric methods for measuring the monophenolase and diphenolase activities of tyrosinase. *J. Agric. Food Chem.* **2007**, *55*, 9739–9749.

Received for review May 2, 2008. Revised manuscript received December 23, 2008. Accepted December 26, 2008. This paper was partially supported by grants from the Ministerio de Educación y Ciencia (Madrid, Spain) Project BIO2006-15363 and SAF 2006-07040-C02-01 from the Fundación Séneca (CARM, Murcia, Spain) Project 00672/PI/04, and from the Consejería de Educación (CARM, Murcia, Spain) BIO-BMC 06/01-0004. F.G.M. has a fellowship from Fundación Caja Murcia (Murcia, Spain). J.L.M.-M. has a fellowship from the Ministerio de Educación y Ciencia (Madrid, Spain), Reference AP2005-4721.

JF803447G